Jin *et al. J Wireless Com Network* (2021) 2021:144
https://doi.org/10.1186/s13638-021-02020-3

EURASIP Journal on Wireless Communications and Networking

RESEARCH Open Access

Physical layer security transmission scheme based on artificial noise in cooperative SWIPT NOMA system

Yong Jin, Zhentao Hu*, Dongdong Xie, Guodong Wu and Lin Zhou

*Correspondence:
hzt@henu.edu.cn
School of Computer and Information Engineering, Henan University, Kaifeng, China

Abstract

Aiming at high energy consumption and information security problem in the simultaneous wireless information and power transfer (SWIPT) multi-user wiretap network, we propose a user-aided cooperative non-orthogonal multiple access (NOMA) physical layer security transmission scheme to minimize base station (BS) transmitted power in this paper. In this scheme, the user near from BS is adopted as a friendly relay to improve performance of user far from BS. An energy harvesting (EH) technology-based SWIPT is employed at the near user to collect energy which can be used at cooperative stage. Since eavesdropper in the downlink of NOMA system may use successive interference cancellation (SIC) technology to obtain the secrecy information of receiver, to tackle this problem, artificial noise (AN) is used at the BS to enhance security performance of secrecy information. Moreover, semidefinite relaxation (SDR) method and successive convex approximation (SCA) technique are combined to solve the above non-convex problem. Simulation results show that in comparison with other methods, our method can effectively reduce the transmitted power of the BS on the constraints of a certain level of the secrecy rates of two users.

Keywords: SWIPT, NOMA, Power splitting (PS), Secrecy communication, AN

1 Introduction

High-speed transmission rates of smart terminals in fifth-generation (5G) wireless communication systems require vast spectrum resources [1, 2]. Traditional orthogonal multiple access (OMA) approaches are difficult to meet the needs of high-speed, real-time and wide-bandwidth in 5G. Researchers proposed NOMA technique, one of the key technologies of 5G, to provide higher spectral efficiency (SE) of multiple users. Keypoint of NOMA is multiple non-orthogonal access of power domain. Thus, multiple users can be served by the same resource block (time domain, frequency domain and code domain). However, due to mutual interference of non-orthogonal signal, the receiver has to use the SIC technique to extract desired information from received signal [3–5].

For the purpose of improving the performance of NOMA, the mode of effectively combining NOMA and cooperative technique has been attracted great attentions. The existing cooperative NOMA mainly can be divided into two types including the

user-assisted and the relay-assisted. For example, J. Men and J. Ge explored the outage probability of the cooperative NOMA relay network by deriving a closed-form expression [6]. A two-stage relay selection scheme was presented to research the outage performance of the cooperative NOMA system in [7–9]. Z. Ding proposed a half-duplex user-aided cooperative NOMA scheme to achieve the maximum diversity gain, and the simulation results indicate that the proposed cooperative NOMA scheme could improve the outage probability [10]. S. L. Talbot and B. Farhang-Boroujeny presented a cooperative beamforming NOMA scheme which performed intrabeam superposition coding of a multi-user signal at the transmitter and the spatial filtering of interbeam interference followed by the intrabeam SIC at the destination [11].

In addition, energy efficiency (EE) is another concern of 5G. Since radio frequency (RF) signals can carry information and transmit energy simultaneously, they can be used not only for information vehicle but also for energy collection of the system. At present, a technology which can effectively extend the service life of energy-limited device called SWIPT has been proposed [12]. Different from traditional EH technologies, such as solar and wind, SWIPT provides stable and controllable energy for wireless applications while transmitting the necessary information contained in RF signal. For this reason, there are many relevant studies on SWIPT that have been appeared in the recent several years. Early studies on SWIPT have assumed that the entire signal can transmit both information and energy, exposing a fundamental trade-off between power and information transfer [13]. But this simultaneous transfer is unrealistic, since the EH operation employed in the RF domain destroys the information content. In order to practically achieve SWIPT, the received signal has to be allocated into two distinct parts, one for information decoding and another for EH [14]. Specifically, Zhang proposed two practical receiver architectures to handle the technical limitations of existing circuit designs, namely time-switching (TS) receiver and PS receiver. If TS is performed, the receiver switches in time between EH and information decoding. In this case, signal allocating is employed in the time domain. So, the entire signal received in one time slot is used either for EH or information decoding. The TS scheme allows for a simple hardware implementation at the receiver but requires accurate time synchronization. The PS scheme has higher receiver complexity compared to TS and requires the optimization of the PS factor [15]. However, Krikidis and Timotheou indicated that the PS technology achieves lower outage probability and higher gain than those of TS for applications with delay constraints. It is intuitive since the signal received in one time slot is used for both power transfer and information decoding when the PS protocol is performed. [14]. In order to further meet practical scenario, in contrast to the most of existing works which apply an ideally linear EH model, Zhou and Chu adopted the practical nonlinear EH model to capture the nonlinear characteristics of EH circuits and designed the resource allocation schemes for SWIPT networks[16].

Motivated by the requirements of 5G and the advantages of NOMA and SWIPT, using SWIPT to enhance SE and EE in NOMA system which contains energy-limited devices is a hotspot today [17].Liu and Ding introduce SWIPT into NOMA system to extend self-sustaining time of system. This strategy employs the near users as EH relays to improve communication quality of far users. Outage rates with respect to three kinds of relay selection schemes are evaluated in single-input single-output (SISO) scenario.

The analytical results demonstrate that SWIPT technology can effectively enhance EE of conventional NOMA systems without jeopardizing its diversity gain [18]. Xu and Ding proposed a SWIPT NOMA cooperative transmission strategy to design a joint beamformer and power-distribution in multi-input single-output (MISO) scene with the perfect channel state information (CSI) model [19]. Furthermore, a joint design of the PS ratio and beamformer was studied in the imperfect CSI model [20]. However, the security of cooperative transmission is not involved in their work. Thus, the private information is easily intercepted and eavesdropped from open wireless channel [21, 22]. To overcome this issue, the cooperative jamming (CJ) technique can be introduced for transmitting AN to degrade the quality of the wiretap link. The existing CJ technique mainly can be classified into three different types including the source-aided CJ, relay-aided CJ and the destination-aided CJ. The source-aided CJ refers to combining information bearing signal with AN injected by the source [23]. In order to improve security of network, Moradikia et al. employed the AN which is injected by the idle transmitter in the scene of untrusted relays and passive eavesdroppers existing [24]. The relay-aided CJ describes the relay nodes of the system chosen to work as a jammer [25]. Liu Y combined cooperative relay with CJ technique to interfere eavesdropper. The research shows that their method can effectively improve the secrecy rate [26]. Zhou and Chu used AN technique to improve the information security of users in the SWIPT NOMA system which has an untrusted energy harvesting receiver [27]. The destination-aided CJ considers the AN transmitted by the destination [28]. A novel cooperative secure unmanned aerial vehicle-assisted propagation protocol has been presented by M. Tatar Mamaghani. For the purpose of enhancing physical-layer security and propagation reliability, they employed destination-assisted CJ as well as SWIPT at the unmanned aerial vehicle mounted relay [29]. Furthermore, Hu Z explored physical layer security of SWIPT relay network with imperfect the CSI model. An algorithm is presented to optimize secret rate of SWIPT network in the constraints of relay forward power and eavesdroppers SINR [30]. Cao and Wang studied the security transmission of uplink NOMA with the aid of the EH receivers. One of the EH receivers is selected as a friendly jammer that adopts the energy harvested from the RF signals to transmit the AN for interfering the eavesdropper [31]. However, the collaboration secrecy scheme of SWIPT and NOMA is not involved in their work. Thus, it motivates us to use AN-aided cooperative strategy to enhance physical-layer security of MISO SWIPT NOMA system. The main contributions of this paper are summarized as follows.

- We propose a source-aided CJ SWIPT NOMA strategy, where the near user serves as an EH relay to help the far user to improve the secrecy rate. By applying the PS protocol, the near user can simultaneously receive information and harvest energy used for the forwarding stage. In addition, multiple antennas and AN-aided techniques are exploited to protect the private information.
- The above scheme can be described as the problem of minimizing transmitted power from BS subject to secrecy rate of each user. To tackle this problem, we need to jointly optimize beamforming vector, AN covariance matrix and PS ratio. Unfortunately, it is NP-hard. So, variable slack technique is combined with SCA method to get suboptimal solution of the original problem. The simulation results verify the

proposed scheme which not only guarantees information security but also reduces BS's energy consumption.

The paper is organized as follows. In Sect. 2, we first introduce the system model and the problem formulation of the cooperative SWIPT NOMA in MISO system. Next, an SCA-based iterative algorithm is proposed to solve the joint AN-aided beamforming design and power splitting control problem. Then, we present numerical results on the performance of different schemes in Sect. 3. Finally, we conclude the paper in Sect. 4.

Notations: Boldface capital letters and boldface lowercase letters denote matrices and vectors, respectively. $\mathbb{C}$ represents the complex domain. $\mathbb{E}|\cdot|$ denotes the expectation operator. The superscript $(\cdot)^T$ and $(\cdot)^H$ denote the transpose and (Hermitian) conjugate transpose, respectively. $\mathrm{Tr}(\cdot)$ represents the trace of a matrix. $||\cdot||$ denotes the magnitude of a complex number. $\mathcal{CN}(\mathbf{0}, \mathbf{X})$ denotes the circularly symmetric complex Gaussian distribution with mean vector $\mathbf{0}$ and covariance matrix $\mathbf{X}$.

2 Methods/experimental

2.1 System model and problem formulation

Consider a downlink in an MISO system is depicted in Fig. 1. BS is equipped with N_t antennas. Two users and a passive eavesdropper are equipped with a single antenna, respectively. For simplicity, supposing eavesdropper and user 2 do not have a direct link, and the eavesdropper is distributed outside the security area center on user 2 near from BS (eavesdropper in the security will be detected by user 2). Similar to reference [32], we assume that some handshaking mechanisms are introduced in the medium access control (MAC) protocol of user 1 and user 2 to inhibit the interception occurring in the security area center on user 2. Specifically, user 1 and user 2 can employ a particular MAC protocol to exchange data while the eavesdropper without MAC protocol may only intercept the data from the BS without MAC protocol. Assume that the channel quality of the user 2 and the eavesdropper is better than that of user 1, respectively. For example, consider an indoor sensor communication scenario where user 2 and eavesdropper are closer to the BS than user 1.

Cooperative SWIPT NOMA transmission scheme is divided into two phases. In the first phase, the eavesdropper intercepts the transmitted signal from BS, and user 1 receives the transmitted signal from BS while user 2 performs SWIPT technique based

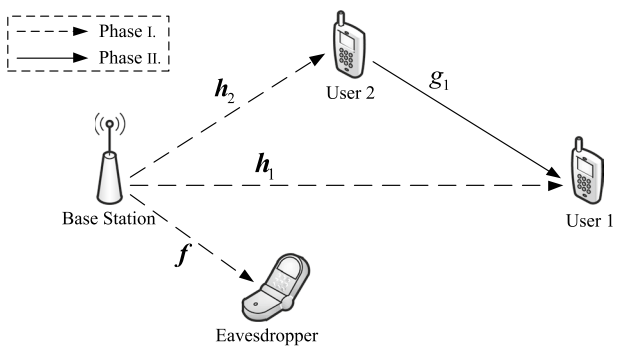

Fig. 1 The system model

on PS protocol. The PS protocol achieves SWIPT by allocating the received radio frequency signal at the user 2 into two streams of different power levels using a PS factor: one signal stream is converted to baseband for information decoding, and the other is sent to the rectenna circuit for EH. Assume that the harvested energy at the user 2 is only used for information forwarding at the second stage, while the energy for maintaining circuit, signal processing, etc., is neglected. When the harvested energy is more than the energy needed to information forwarding at user 2, there is an energy buffer at the secondary transmitter to store the excess energy. In the second phase, user 2 uses harvested energy in phase 1 to forward the message received in phase 1 to user 1, while user 1 employs maximal-ratio combination (MRC) criterion to accumulate and decode the messages received in two phases. Since the eavesdropper is distributed outside the security area center on user 2 near from BS, eavesdropper cannot receive the transmitted signal from user 2. Details of the process are presented next.

In the first transmission phase, in order to improve the security of the BS's transmitted signal and reduce the risk of information leakage, an AN vector $\mathbf{v} \in \mathbb{C}^{N_t}$ is added to the transmitted signal. Therefore, the transmitted signal from the BS is described as $\mathbf{s} = \mathbf{w}_1 s_1 + \mathbf{w}_2 s_2 + \mathbf{v}$, where $s_1, s_2 \in \mathbb{C}$ are information bearing messages for user 1 and user 2, respectively. And $\mathbf{w}_1, \mathbf{w}_2 \in \mathbb{C}^{N_t}$ are the corresponding transmitted beamformers. We assume that the power of the transmitted symbol is normalized, i.e., $\mathbb{E}|s_1|^2 = \mathbb{E}|s_2|^2 = 1$, and the AN vector $\mathbf{v} \sim \mathcal{CN}(\mathbf{0}, \mathbf{S})$, where $\mathbf{S}$ is the covariance matrix of AN to be designed. Then, the signal received at user 1 is given by

$$y_1^{(1)} = \widetilde{\mathbf{h}}_1^H(\mathbf{w}_1 s_1 + \mathbf{w}_2 s_2 + \mathbf{v}) + n_1^{(1)}, \tag{1}$$

where $\widetilde{\mathbf{h}}_1^H \in \mathbb{C}^{N_t}$ is the channel impulse response vector between the BS and user 1, and $n_1^{(1)} \sim \mathcal{CN}(0, \sigma_1^2)$ represents the additive Gaussian white noise (AWGN) at user 1. Then, the signal-to-interference-plus-noise-ratio (SINR) received by user 1 for s_1 can be expressed as

$$\mathrm{SINR}_1^{(1)} = \frac{|\widetilde{\mathbf{h}}_1^{\mathrm{H}}\mathbf{w}_1|^2}{|\widetilde{\mathbf{h}}_1^{\mathrm{H}}\mathbf{w}_2|^2 + |\widetilde{\mathbf{h}}_1^{\mathrm{H}}\mathbf{v}|^2 + \sigma_1^2}, \tag{2}$$

by defining $\mathbf{h}_1 = \widetilde{\mathbf{h}}_1/\sigma_1$, (2) is transformed as

$$\mathrm{SINR}_1^{(1)} = \frac{\mathbf{h}_1^{\mathrm{H}}\mathbf{w}_1\mathbf{w}_1^{\mathrm{H}}\mathbf{h}_1}{\mathbf{h}_1^{\mathrm{H}}\big(\mathbf{w}_2\mathbf{w}_2^{\mathrm{H}} + \mathbf{S}\big)\mathbf{h}_1 + 1}. \tag{3}$$

As shown in Fig. 2, the power splitting architecture with respect to user 2, is introduced to perform SWIPT. Hence, the received signal for information decoding at user 2 can be described as

$$y_2^{(1)} = \sqrt{1-\rho}\widetilde{\mathbf{h}}_2^H(\mathbf{w}_1 s_1 + \mathbf{w}_2 s_2 + \mathbf{v}) + n_2^{(1)}, \tag{4}$$

where $\rho \in [0, 1]$ is the PS ratio of energy harvesting to be optimized later, $\widetilde{\mathbf{h}}_2^H \in \mathbb{C}^{N_t}$ is the channel impulse response vector between the BS and user 2, $n_2^{(1)} \sim \mathcal{CN}(0, \sigma_2^2)$ represents the AWGN.

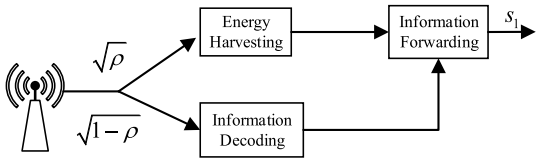

Fig. 2 The power splitting architecture at user 2

According to the NOMA principle, SIC is performed at user 2. Specifically, user 2 first decodes user 1's message (i.e., s_1) and then subtracts this message from the received signal to decode its own message [33]. Therefore, the SINR received at user 2 to decode s_1 can be expressed as

$$\mathrm{SINR}_{2,s_1}^{(1)} = \frac{(1-\rho)\mathbf{h}_2^{\mathrm{H}}\mathbf{w}_1\mathbf{w}_1^{\mathrm{H}}\mathbf{h}_2}{(1-\rho)\mathbf{h}_2^{\mathrm{H}}\left(\mathbf{w}_2\mathbf{w}_2^{\mathrm{H}}+\mathbf{S}\right)\mathbf{h}_2+1}, \tag{5}$$

where $\mathbf{h}_2 = \widetilde{\mathbf{h}}_2/\sigma_2$.

Then, user 2 subtracts s_1 from $y_2^{(1)}$ to further decode its own message s_2. The corresponding SINR can be described as

$$\mathrm{SINR}_{2,s_2}^{(1)} = \frac{(1-\rho)\mathbf{h}_2^{\mathrm{H}}\mathbf{w}_2\mathbf{w}_2^{\mathrm{H}}\mathbf{h}_2}{(1-\rho)\mathbf{h}_2^{\mathrm{H}}\mathbf{S}\mathbf{h}_2+1}. \tag{6}$$

On the other hand, the energy harvested by user 2 is modeled as [34]

$$E = \rho\left(|\widetilde{\mathbf{h}}_2^H\mathbf{w}_1|^2 + |\widetilde{\mathbf{h}}_2^H\mathbf{w}_2|^2 + |\widetilde{\mathbf{h}}_2^H\mathbf{v}|^2\right)\eta, \tag{7}$$

where η is the ratio of the first phase in a transmission time slot, and we assume that the two phases have the same transmission duration, then $\eta = 0.5$.

Thus, in the second phase, the transmitted power of user 2 related to forwarding messages is

$$P_t = \frac{E}{1-\eta} = \rho\left(|\widetilde{\mathbf{h}}_2^H\mathbf{w}_1|^2 + |\widetilde{\mathbf{h}}_2^H\mathbf{w}_2|^2 + |\widetilde{\mathbf{h}}_2^H\mathbf{v}|^2\right). \tag{8}$$

In addition, the signal received at the eavesdropper can be expressed as

$$y_e^{(1)} = \widetilde{\mathbf{f}}^H(\mathbf{w}_1 s_1 + \mathbf{w}_2 s_2 + \mathbf{v}) + n_e^{(1)}, \tag{9}$$

where $\widetilde{\mathbf{f}}^H \in \mathbb{C}^{N_t}$ is the channel impulse response vector between the BS and eavesdropper, and $n_e^{(1)} \sim \mathcal{CN}(0, \sigma_e^2)$ represents the AWGN at eavesdropper. Then, the SINR received by eavesdropper for the message s_1 can be expressed as

$$\mathrm{SINR}_{\mathrm{e},s_1}^{(1)} = \frac{\mathbf{f}^{\mathrm{H}}\mathbf{w}_1\mathbf{w}_1^{\mathrm{H}}\mathbf{f}}{\mathbf{f}^{\mathrm{H}}\left(\mathbf{w}_2\mathbf{w}_2^{\mathrm{H}}+\mathbf{S}\right)\mathbf{f}+1}. \tag{10}$$

where $\mathbf{f} = \widetilde{\mathbf{f}}/\sigma_e$.

The eavesdropper then performs the SIC, subtracts s_1 from its signal to further decode the other message s_2. The corresponding SINR can be described as

$$\mathrm{SINR}_{\mathrm{e},s_2}^{(1)} = \frac{\mathbf{f}^{\mathrm{H}}\mathbf{w}_2\mathbf{w}_2^{\mathrm{H}}\mathbf{f}}{\mathbf{f}^{\mathrm{H}}\mathbf{S}\mathbf{f}+1}. \tag{11}$$

In the second phase, user 2 forwards the message to user 1 with the harvested energy. At this point, the signal received at user 1 is

$$y_1^{(2)} = \sqrt{P_t}g_1 s_1 + n_1^{(2)}, \tag{12}$$

where $g_1 \in \mathbb{C}$ is the channel coefficient from user 2 to user 1, and $n_1^{(2)} \sim \mathcal{CN}(0,\sigma_1^2)$ is the AWGN at user 1. Note that we consider the case of $\sigma_1^2 = \sigma_2^2$ for the simplicity of exposition. Thus, the SINR received by user 1 for s_1 can be given by

$$\mathrm{SINR}_{1,s_1}^{(2)} = \rho g\Big(\mathbf{h}_2^{\mathrm{H}}(\mathbf{w}_1\mathbf{w}_1^{\mathrm{H}} + \mathbf{w}_2\mathbf{w}_2^{\mathrm{H}} + \mathbf{S})\mathbf{h}_2\Big), \tag{13}$$

where $g = |g_1|^2$.

In communication systems, MRC usually be performed following synchronization, channel estimation and channel equalization (in the sampling domain). Since synchronization, channel estimation and channel equalization are not main concerns in this paper, similar as reference[19] and[35], we assume each channel has been completely synchronized before performing the MRC. So, user 1 can combine the signals received from the BS and the user 2 to jointly decode the message. The equivalent SINR at user 1 can be written as

$$\begin{aligned}\mathrm{SINR}_{1,s_1} =& \quad \mathrm{SINR}_1^{(1)} + \mathrm{SNR}_{1,s_1}^{(2)} \\ =& \frac{\mathbf{h}_1^H\mathbf{w}_1\mathbf{w}_1^H\mathbf{h}_1}{\mathbf{h}_1^H(\mathbf{w}_2\mathbf{w}_2^H + \mathbf{S})\mathbf{h}_1 + 1} + \rho g\big(\mathbf{h}_2^H(\mathbf{w}_1\mathbf{w}_1^H + \mathbf{w}_2\mathbf{w}_2^H + \mathbf{S})\mathbf{h}_2\big).\end{aligned} \tag{14}$$

Therefore, according to the SINR of the legitimate user and the eavesdropper, the secrecy rate R_1 and secrecy rate R_2 of the user 1 and the user 2 are defined as follows

$$\begin{aligned}R_1 =& \min\Big\{0.5\log_2\big(1+\mathrm{SINR}_{1,s_1}\big), 0.5\log_2\Big(1+\mathrm{SINR}_{2,s_1}^{(1)}\Big)\Big\} \\ &- 0.5\log_2\Big(1+\mathrm{SINR}_{\mathrm{e},s_1}^{(1)}\Big)\end{aligned} \tag{15a}$$

$$R_2 = 0.5\log_2\Big(1+\mathrm{SINR}_{2,s_2}^{(1)}\Big) - 0.5\log_2\Big(1+\mathrm{SINR}_{\mathrm{e},s_2}^{(1)}\Big). \tag{15b}$$

we want to minimize the transmitted power of the BS while guaranteeing the level of secrecy rates related to users. The optimization problem can be expressed as follow

$$\mathbf{P}_1 : \min_{\rho,\mathbf{w}_1,\mathbf{w}_2,\mathbf{S}} \mathrm{Tr}\big(\mathbf{w}_1\mathbf{w}_1^H + \mathbf{w}_2\mathbf{w}_2^H + \mathbf{S}\big) \tag{16a}$$

$$\text{s.t. } C0 : R_1 \geq \gamma_1, \tag{16b}$$

$$C1 : R_2 \geq \gamma_2, \tag{16c}$$

$$C2: 0 \leq \rho < 1, \tag{16d}$$

$$C3: \mathbf{S} \succeq 0, \tag{16e}$$

where γ_1 and γ_2 represent the minimum required secret rate thresholds with respect to user 1 and user 2, respectively. The constraint $C0$ is to ensure s_1 can be successfully decoded at user 2 meanwhile guarantee the SINR requirement of user 1 satisfied, and the constraint $C1$ ensures the secure transmission of message s_2 at user 2. Observing equ (15.a) and equ (15.b), we can find that ρ, $\mathbf{w}_1$ and $\mathbf{w}_2$ are coupled together in the R_1 and R_2. Thus, P1 is a nonconvex problem and is difficult to solve. In the following, we will firstly employ SDR technique to reformulate P1 and then approximately solve the reformulated problem with an SCA-based iterative algorithm.

$$\begin{aligned}
R_{1,s_1} &= \frac{[\mathrm{Tr}((\mathbf{W}_1+\mathbf{W}_2+\mathbf{S})\mathbf{F})+1]}{\left\{\frac{[\mathrm{Tr}((\mathbf{W}_1+\mathbf{W}_2+\mathbf{S})\mathbf{H}_1)+1]}{[\mathrm{Tr}((\mathbf{W}_2+\mathbf{S})\mathbf{H}_2)+1]}+\rho g\mathrm{Tr}((\mathbf{W}_1+\mathbf{W}_2+\mathbf{S})\mathbf{H}_2)\right\}[\mathrm{Tr}((\mathbf{W}_2+\mathbf{S})\mathbf{F})+1]} \\
R_{2,s_1} &= \frac{[(1-\rho)\mathrm{Tr}((\mathbf{W}_2+\mathbf{S})\mathbf{H}_2)+1][\mathrm{Tr}((\mathbf{W}_1+\mathbf{W}_2+\mathbf{S})\mathbf{F})+1]}{[(1-\rho)\mathrm{Tr}((\mathbf{W}_1+\mathbf{W}_2+\mathbf{S})\mathbf{H}_2)+1][\mathrm{Tr}((\mathbf{W}_2+\mathbf{S})\mathbf{F})+1]} \\
R_{2,s_2} &= \frac{[(1-\rho)\mathrm{Tr}(\mathbf{S}\mathbf{H}_2)+1][\mathrm{Tr}((\mathbf{W}_2+\mathbf{S})\mathbf{F})+1]}{[(1-\rho)\mathrm{Tr}((\mathbf{W}_2+\mathbf{S})\mathbf{H}_2)+1][\mathrm{Tr}(\mathbf{S}\mathbf{F})+1]}
\end{aligned} \tag{17}$$

2.2 AN-aided beamforming design and power splitting control

Let $\mathbf{W}_1 = \mathbf{w}_1\mathbf{w}_1^H$, $\mathbf{W}_2 = \mathbf{w}_2\mathbf{w}_2^H$ and drop rank-one constraints $\mathrm{rank}(\mathbf{W}_1) = 1$, $\mathrm{rank}(\mathbf{W}_2) = 1$. P1 can be relaxed to P2, given as

$$\mathbf{P}_2: \min_{\rho,\mathbf{W}_1,\mathbf{W}_2,\mathbf{S}} \mathrm{Tr}(\mathbf{W}_1+\mathbf{W}_2+\mathbf{S}) \tag{18a}$$

$$\text{s.t.} \quad C4: R_{1,s_1} \leqslant 2^{-\gamma_1}, \tag{18b}$$

$$C5: R_{2,s_1} \leqslant 2^{-\gamma_1}, \tag{18c}$$

$$C6: R_{2,s_2} \leqslant 2^{-\gamma_2}, \tag{18d}$$

$$C7: 0 \leq \rho < 1, \tag{18e}$$

$$C8: \mathbf{S} \succeq 0, \mathbf{W}_1 \succeq 0, \mathbf{W}_2 \succeq 0, \tag{18f}$$

where $\mathbf{H}_1 \triangleq \mathbf{h}_1\mathbf{h}_1^H$, $\mathbf{H}_2 \triangleq \mathbf{h}_2\mathbf{h}_2^H$ and $\mathbf{F} \triangleq \mathbf{f}\mathbf{f}^H$. Moreover, R_{1,s_1} and R_{2,s_1} represent the secrecy rates of message s_1 at user 1 and user 2, respectively. R_{2,s_2} represents that of message s_2 at user 2(c.f. (17)). Due to the constraints $C4$, $C5$ and $C6$ are still non-convex, they are converted to the following equivalent by introducing exponential auxiliary variables [36]. The constraint $C4$ is equivalently expressed as

$$\exp\left(x_1 - y_1 - y_2\right) \leqslant 2^{-\gamma_1}, \tag{19a}$$

$$\mathrm{Tr}((\mathbf{W}_1+\mathbf{W}_2+\mathbf{S})\mathbf{F})+1\leqslant \exp(x_1), \tag{19b}$$

$$\frac{[\mathrm{Tr}((\mathbf{W}_1+\mathbf{W}_2+\mathbf{S})\mathbf{H}_1)+1]}{[\mathrm{Tr}((\mathbf{W}_2+\mathbf{S})\mathbf{H}_1)+1]}+\rho g\mathrm{Tr}((\mathbf{W}_1+\mathbf{W}_2+\mathbf{S})\mathbf{H}_2)\geqslant \exp\left(y_1\right), \tag{19c}$$

$$\mathrm{Tr}((\mathbf{W}_2+\mathbf{S})\mathbf{F})+1\geqslant \exp\left(y_2\right), \tag{19d}$$

where x_1, y_1, y_2 are exponential auxiliary variables. Here, only (19b) and (19c) remain as non-convex constraints. By using the first-order Taylor expansion approximation, the non-convex constraint (19b) can be approximated as

$$\mathrm{Tr}((\mathbf{W}_1+\mathbf{W}_2+\mathbf{S})\mathbf{F})+1\leqslant \exp\left(\widetilde{x_1}\right)\left(x_1-\widetilde{x_1}+1\right), \tag{20}$$

where $\widetilde{x}_1$ is an approximate value, and it is equal to x_1, when the corresponding constraints are tight.

Furthermore, by introducing an auxiliary variable $x_2\geqslant 0$, constraint (19c) can be equivalently expressed as

$$\mathrm{Tr}((\mathbf{W}_1+\mathbf{W}_2+\mathbf{S})\mathbf{H}_1)\geqslant x_2\mathrm{Tr}((\mathbf{W}_2+\mathbf{S})\mathbf{H}_1)+x_2-1, \tag{21a}$$

$$\rho g\mathrm{Tr}((\mathbf{W}_1+\mathbf{W}_2+\mathbf{S})\mathbf{H}_2)\geqslant \exp\left(y_1\right)-x_2. \tag{21b}$$

For constraint (21a), an approximate convex constraint is produced by using the arithmetic-geometric mean (AGM) inequality $xy\leqslant z$. That is, for any nonnegative variable x, y and z, if and only if $a=\sqrt{y/x}$, the following formula holds

$$2xy\leqslant (ax)^2+(y/a)^2\leqslant 2z. \tag{22}$$

Therefore, constraint (21a) is approximated by a convex constraint as follows

$$\left(\widetilde{a}_1x_2\right)^2+\left(\mathrm{Tr}((\mathbf{W}_2+\mathbf{S})\mathbf{H}_1)/\widetilde{a}_1\right)^2\leqslant 2\mathrm{Tr}((\mathbf{W}_1+\mathbf{W}_2+\mathbf{S})\mathbf{H}_1)+2-2x_2, \tag{23}$$

where $\widetilde{a}_1$ is an approximate value, which is updated after each iteration by the following formula

$$\widetilde{a}_1=\sqrt{\mathrm{Tr}((\mathbf{W}_2+\mathbf{S})\mathbf{H}_1)/x_2}. \tag{24}$$

Using epigraph reformulation [37], the constraint (21b) can be transformed into a non-convex quadratic constraint and a convex LMI constraint as below

$$u^2\geqslant \exp(y_1)-x_2, \tag{25a}$$

$$\begin{bmatrix} g\rho & u \\ u & \mathrm{Tr}((\mathbf{W}_1+\mathbf{W}_2+\mathbf{S})\mathbf{H}_2)\end{bmatrix}\succeq 0. \tag{25b}$$

And then, the non-convex quadratic inequality constraint (25a) is still approximated by Taylor expansion as

$$2\widetilde{u}u - \widetilde{u}^2 \geqslant \exp(y_1) - x_2, \tag{26}$$

where $\widetilde{u}$ is an approximate value.

Similar to *C*4, constraint *C*5 is approximated as

$$\exp\left(x_3 + x_4 - y_3 - y_4\right) \leqslant 2^{-\gamma_1}, \tag{27a}$$

$$\left(\widetilde{a}_2(1-\rho)\right)^2 + \left(\mathrm{Tr}((\mathbf{W}_2 + \mathbf{S})\mathbf{H}_2)/\widetilde{a}_2\right)^2 \leqslant 2\exp\left(\widetilde{x_3}\right)\left(x_3 - \widetilde{x_3} + 1\right) - 2, \tag{27b}$$

$$\mathrm{Tr}((\mathbf{W}_1 + \mathbf{W}_2 + \mathbf{S})\mathbf{F}) + 1 \leqslant \exp\left(\widetilde{x_4}\right)\left(x_4 - \widetilde{x_4} + 1\right), \tag{27c}$$

$$2\widetilde{t}t - \widetilde{t}^2 + 1 \geqslant \exp\left(y_3\right), \tag{27d}$$

$$\begin{bmatrix} 1-\rho & t \\ t & \mathrm{Tr}((\mathbf{W}_1 + \mathbf{W}_2 + \mathbf{S})\mathbf{H}_2) \end{bmatrix} \succeq 0, \tag{27e}$$

$$\mathrm{Tr}((\mathbf{W}_2 + \mathbf{S})\mathbf{F}) + 1 \geqslant \exp(y_4). \tag{27f}$$

where $\widetilde{x}_3$, $\widetilde{x}_4$, $\widetilde{t}$ and $\widetilde{a}_2$ are approximate values. In addition, $\widetilde{a}_2$ is updated after each iteration by the following formula

$$\widetilde{a}_2 = \sqrt{\mathrm{Tr}((\mathbf{W}_2 + \mathbf{S})\mathbf{H}_2)/(1-\rho)} \tag{28}$$

Similar to *C*5, constraint *C*6 is approximated as

$$\exp\left(x_5 + x_6 - y_5 - y_6\right) \leqslant 2^{-\gamma_2}, \tag{29a}$$

$$\left(\widetilde{a}_3(1-\rho)\right)^2 + \left(\mathrm{Tr}(\mathbf{S}\mathbf{H}_2)/\widetilde{a}_3\right)^2 \leqslant 2\exp(\widetilde{x}_5)(x_5 - \widetilde{x}_5 + 1) - 2, \tag{29b}$$

$$\mathrm{Tr}((\mathbf{W}_2 + \mathbf{S})\mathbf{F}) + 1 \leqslant \exp(\widetilde{x}_6)(x_6 - \widetilde{x}_6 + 1), \tag{29c}$$

$$2\widetilde{q}q - \widetilde{q}^2 + 1 \geqslant \exp(y_5), \tag{29d}$$

$$\begin{bmatrix} 1-\rho & q \\ q & \mathrm{Tr}((\mathbf{W}_2 + \mathbf{S})\mathbf{H}_2) \end{bmatrix} \succeq 0, \tag{29e}$$

$$\mathrm{Tr}(\mathbf{S}\mathbf{F}) + 1 \geqslant \exp(y_6). \tag{29f}$$

where $\widetilde{x}_5$, $\widetilde{x}_6$, $\widetilde{q}$ and $\widetilde{a}_3$ are approximate values. Moreover, $\widetilde{a}_3$ is updated after each iteration by the following formula

$$\widetilde{a}_3 = \sqrt{\mathrm{Tr}(\mathbf{S}\mathbf{H}_2)/(1-\rho)}. \tag{30}$$

Therefore, P2 can be approximated as P3 as follows

$$\begin{aligned}\mathbf{P}_3: \min_{\rho,\mathbf{W}_1,\mathbf{W}_2,\mathbf{S},x_i,y_i,u,t,q} \ & \mathrm{Tr}(\mathbf{W}_1+\mathbf{W}_2+\mathbf{S}) \\ \text{s.t.} \ & (18e),(18f)(19a),(19d),(20),(23),(25b),(26),(27),(29)\end{aligned} \tag{31}$$

where $i \in \{1,2,3,4,5,6\}$. We can see that P3 is a standard convex optimization problem. According to the solution of P3, an iterative algorithm using SCA can be developed to solve P1, the specific solution process is shown in Table 1. In addition, if the solution $(\mathbf{W}_1^*, \mathbf{W}_2^*)$ yielded by SDR is rank-one, then the optimal beamforming vectors $\mathbf{w}_1^*$ and $\mathbf{w}_2^*$ are obtained by eigenvalue-decomposition of $\mathbf{W}_1^*$ and $\mathbf{W}_2^*$, respectively. Otherwise, the suboptimal solution can be yielded by using Gaussian randomization procedure [38].

3 Results and discussion

In this section, some simulation results are shown to demonstrate the performance of the proposed AN-aided cooperate SWIPT NOMA transmission scheme. Consider that two legitimate users and a passive eavesdropper (located outside of the "security zone") are randomly deployed in an $5m \times 6m$ area, and the BS is fixed at the edge with a coordinate $(0m, 2.5m)$. This scenario is suitable for an indoor sensor communication scenario. $\tilde{h}_1$ is the standard Rayleigh fading coefficient. The distance-dependent path loss is modeled by $P_L = 10^{-3} d^{-\alpha}$, in which d and α denote the Euclidean distance and path loss exponent, respectively. Using the Rician fading channel model, the downlink channels are modeled as

$$\begin{aligned}\widetilde{\mathbf{h}}_2 &= \sqrt{\frac{K}{1+K}}\mathbf{h}_2^{\mathrm{LOS}} + \sqrt{\frac{1}{1+K}}\mathbf{h}_2^{\mathrm{NLOS}} \\ \widetilde{\mathbf{f}} &= \sqrt{\frac{K}{1+K}}\mathbf{f}^{\mathrm{LOS}} + \sqrt{\frac{1}{1+K}}\mathbf{f}^{\mathrm{NLOS}} \\ g_1 &= \sqrt{\frac{K}{1+K}}g_1^{\mathrm{LOS}} + \sqrt{\frac{1}{1+K}}g_1^{\mathrm{NLOS}}\end{aligned}$$

where K denotes the Rician factor, $\mathbf{h}_2^{\mathrm{LOS}}$, $\mathbf{f}^{\mathrm{LOS}}$ and g_1^{LOS} are the line-of-sight (LOS) deterministic components, $\mathbf{h}_2^{\mathrm{NLOS}}$, $\mathbf{f}^{\mathrm{NLOS}}$ and g_1^{NLOS} are the Rayleigh fading components. The detailed simulation parameters are given in Table 2.

We introduce some other transmission strategies, namely the AN-aided NOMA strategy, Non-AN SWIPT NOMA strategy and AN-aided time division multiple access (TDMA) strategy.

- In the AN-aided NOMA strategy, the system still performs the NOMA strategy. However, SWIPT is not executed at user 2, i.e., the cooperative transmission stage is removed in the system. So, in this strategy, power splitting is not to be considered.
- In the Non-AN SWIPT NOMA strategy, we do not add an AN to transmitted signal from the BS in the system. Therefore, AN covariance matrix optimizing is not to be considered in this strategy.
- In the AN-aided TDMA strategy, the system performs the time division multiple access (TDMA) mode, i.e., the BS transmits information to user 1 or user 2 at different dynamic time intervals.

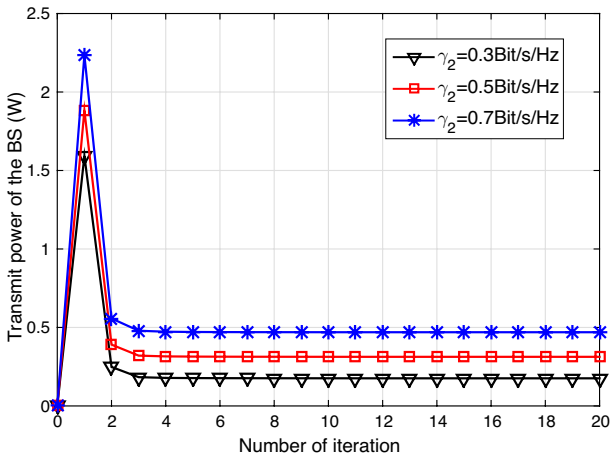

Fig. 3 The minimum transmission power of the BS versus the number of iterations

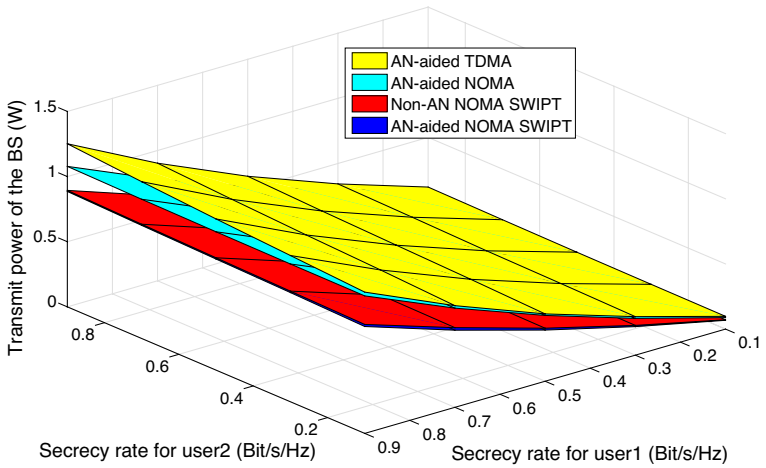

Fig. 4 The minimum transmission power of the BS versus the secrecy rates under different algorithms

Figure 3 describes minimum transmission power of the BS with respect to the number iterations of the proposed algorithm. The minimum required secrecy rate of user 1 is set to be 0.5 Bits/s/Hz. The minimum required secrecy rate of user 2 is set to be 0.3 Bits/s/Hz, 0.5 Bits/s/Hz or 0.7 Bits/s/Hz, respectively. It can be found that only few iterations are required to achieve the minimum transmission power of the BS in all case, which indicates that the proposed algorithm is effective.

Figure 4 shows minimum transmission power of the BS with respect to secrecy rate of user 1 and secrecy rate of user 2, respectively. It can be found that in all cases, NOMA transmission strategies are superior to the TDMA transmission strategy, indicating the advantage of NOMA in improving the system SE. Moreover, our strategy obtains smaller transmission power of the BS than that of other NOMA strategies.

Since user 1 far from BS while user 2 near from BS, their secrecy rates have different impacts on transmission power. Firstly, we analyze the influence of user 1's secrecy

Table 1 The SCA-based algorithm

Algorithm 1 SCA Method for Solving P1

1: **Setting:**

Secrecy rate threshold γ_1 and γ_2,and the tolerance error ξ;

2: **Initialization:**

The iterative number $n = 1$, transmitted power $P_{opt}^{(n)}$,

approximate values $\widetilde{x}_i^{(n)}$, $\widetilde{a}^{(n)}$, $\widetilde{u}^{(n)}$, $\widetilde{t}^{(n)}$ and $\widetilde{q}^{(n)}$;

3: **Repeat:**

Using CVX solver to solve P3 for the given approximate values;

obtain $\widetilde{x}_i^{(n+1)}$, $\widetilde{a}^{(n+1)}$, $\widetilde{u}^{(n+1)}$, $\widetilde{t}^{(n+1)}$ and $\widetilde{q}^{(n+1)}$;

update the iterative number $n = n + 1$;

calculate the total transmitted power $P_{opt}^{(n+1)}$;

if $\left|P_{opt}^{(n+1)} - P_{opt}^{(n)}\right| \leqslant \xi$

break;

end;

4: **Output:**

PS ratio ρ, beamformers $\mathbf{W}_1$ and $\mathbf{W}_2$, AN covariance matrix $\mathbf{S}$.

Table 2 Simulation parameters

Parameters	Notation	Typical values
Numbers of antennas	N_t	2
Variances of noise at user 1	σ_1^2	− 60 dBm
Variances of noise at user 2	σ_2^2	− 60 dBm
Variances of noise at eavesdropper	σ_e^2	− 60 dBm
Distance between BS and user 2	d_2	3 m
Distance between BS and user 1	d_1	5 m
Distance between BS and eavesdropper	d_e	3 m
Distance between user 2 and user 1	d_{12}	2.5 m
Path loss exponent of user 1	α_1	4
Path loss exponent of user 2	α_2	2
Path loss exponent of eavesdropper	α_e	2
Path loss exponent between user 2 and user 1	α_{12}	2
Rician factor	K	3
Channel distribution	$\widetilde{\mathbf{h}}_1$	$\mathcal{CN}(\mathbf{0}, \mathbf{I})$
	$\mathbf{h}_2^{\mathrm{NLOS}}$	$\mathcal{CN}(\mathbf{0}, \mathbf{I})$
	$\mathbf{f}^{\mathrm{NLOS}}$	$\mathcal{CN}(\mathbf{0}, \mathbf{I})$
	g_1^{NLOS}	$\mathcal{CN}(0, \mathrm{I})$

rate on transmission power when the secrecy rate of user 2 was fixed. Again, we analyze the influence of user 2's secrecy rate on transmission power when the secrecy rate of user 1 was fixed.

Figure 5 describes the minimum transmission power of the BS versus the secrecy rate of user 1, where the secrecy rate of user 2 is fixed by 0.5 Bits/s/Hz. Compared with that of other transmission strategies, the transmission power of the proposed AN-aided SWIPT NOMA strategy is the lowest, which demonstrates that the

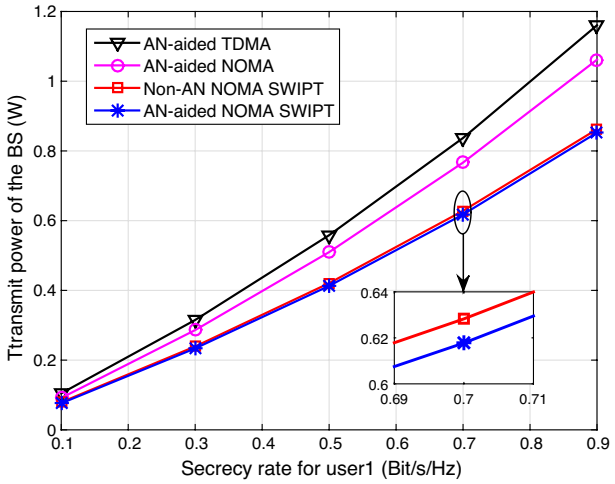

Fig. 5 The minimum transmission power of the BS versus the secrecy rate of user1

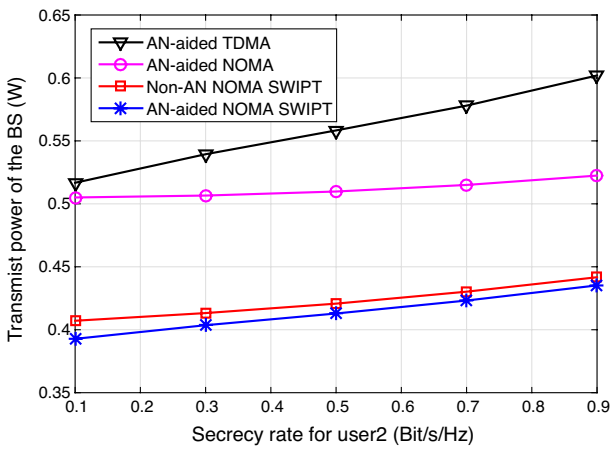

Fig. 6 The minimum transmission power of the BS versus the secrecy rate of user 2

collaboration between SWIPT and NOMA is effective. It is also found that the power of the proposed scheme is slightly lower than that of the Non-AN NOMA SWIPT transmission strategy.

Figure 6 shows the minimum transmission power of the BS versus the secrecy rate of user 2, where the secrecy rate of user 1 is fixed by 0.5 Bits/s/Hz. We observe that the curves of the three NOMA transmission strategies are more smooth than that of TDMA transmission strategy. This indicates that the NOMA transmission strategies are robust with respect to the near user rate, i.e., under the same transmitted power constraint and far user secrecy rate, the NOMA can significantly increase the secrecy rate of the near user compared to that of TDMA. On the other hand, we find that gap of transmission power between AN-aided SWIPT NOMA strategy and AN-aided NOMA strategy decreases gradually with increasing secrecy rate requirement. Moreover, gap of transmission power between AN-aided and Non-AN strategies decreases gradually with increasing the secrecy rate. It clearly demonstrates that gain of user in

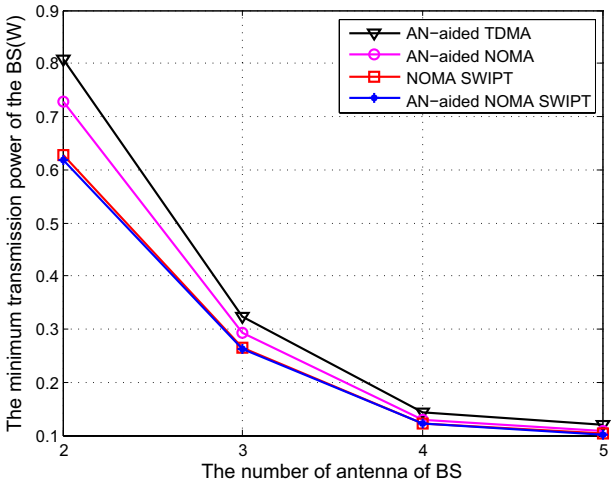

Fig. 7 The minimum transmission power of the BS versus the number of BS's antennas

Table 3 Relationship among PS ratio, secrecy rate of user 1, secrecy rate of user 2

ρ	$\gamma 2$				
$\gamma 1$	**0.1**	**0.3**	**0.5**	**0.7**	**0.9**
0.1	0.5592	0.4014	0.2546	0.1120	0.0077
0.3	0.6417	0.4988	0.3693	0.2387	0.0866
0.5	0.6897	0.5563	0.4381	0.3186	0.1916
0.7	0.7208	0.5943	0.4840	0.3727	0.2521
0.9	0.7468	0.6208	0.5161	0.4110	0.2954

BS caused by SWIPT-cooperative and AN-aided techniques decrease gradually with the increasing of secrecy rate.

Figure 7 describes the minimum transmission power of the BS with respect to the number of BS's antennas, where the secrecy rate of user 1 and the secrecy rate user 2 are fixed by 0.5 Bits/s/Hz. We can find that the transmission power of all methods reduces with the number of BS's antenna. It is intuitive since the diversity gain of system can be enhanced by increasing the number of BS's antennas. Compared with that of TDMA transmission scheme, the transmission power of other three NOMA schemes are lower. This shows that the NOMA transmission schemes are robust. Similar to Fig. 5, it is also found that the power of the proposed scheme is slightly lower than that of the Non-AN NOMA SWIPT transmission strategy.

Table 3 shows the relationship among the PS ratio, the secrecy rate of user 1 and the secrecy rate of user 2. It can be seen that the PS ratio decreases sharply with the user 2's secrecy rate increasing, but increases slowly with the user 1's secrecy rate increasing. This is because the power related to the information decoding of the user 2 is completely determined only by $1-\rho$. Higher secrecy rate requirement of user 2, more power needs to be allocated. Different from that of user 2, the secrecy rate of user 1 is determined by two parts (the transmission signal of the BS and user 2), and thus is less sensitive to the PS ratio than that of user 2.

4 Conclusions

To promote the physical-layer security of the downlink in the MISO system, we propose an AN-aided cooperate SWIPT NOMA strategy. In the scene of one SIC-capable eavesdropper, we explore a cooperative transmission scheme based on multi-antenna, AN-aided, and PS techniques to minimize transmitted power of the BS while satisfying secrecy rate of all legitimate users. This NP-hard problem needs to jointly optimize the beamforming vector of multi-antenna, the covariance matrix of AN-aided and the PS ratio. Thus, we design a suboptimal algorithm by using SDR and SCA techniques to tackle the above NP-hard problem. Simulation studies verify the effectiveness of the proposed transmission scheme.

Abbreviations

NOMA: Non-orthogonal multiple access; SWIPT: Simultaneous wireless information and power transfer; CSI: Channel state information; SIC: Successive interference cancellation; BS: Base station; SDR: Semidefinite relaxation; SCA: Successive convex approximation; PS: Power splitting; AN: Artificial noise; 5G: Fifth-generation; OMA: Orthogonal multiple access; SE: Spectral efficiency; EE: Energy efficiency; RF: Radio frequency; EH: Energy harvesting; TS: Time-switching; CJ: Cooperative jamming; SISO: Single-input single-output; MISO: Multiple-input single-output; MRC: Maximal-ratio combination; AWGN: Additive Gaussian white noise; SINR: Signal-to-interference-noise-ratio; LOS: Line-of-sight; TDMA: Time division multiple access.

Acknowledgements

Not applicable.

Authors' contributions

Y.J was responsible for investigating the AN-aided beamforming design and power splitting control method that are suitable to be implemented. Z.H conceived and designed the study. D.X drafted the manuscript and revised it critically. All authors read and approved the final manuscript.

Funding

This work was supported by the National Science Foundation Council of China (61771006, 61976080), Key research projects of university in Henan Province of China (19A413006, 20B510001), First-class Discipline Training Foundation of Henan University (2018YLTD04), the Programs for Science and Technology Development of Henan Province (192102210254), the Talent Program of Henan University (SYL19060110).

Availability of data and materials

Data sharing not applicable to this paper since no datasets were analyzed during current study.

Declarations

Consent for publication

Not applicable.

Competing interests

The authors declare that they have no competing interests.

Received: 16 November 2020 Accepted: 23 June 2021
Published online: 03 July 2021

References

1. Z. Wei, D. N, J. Yuan, H. Wang, Optimal resource allocation for power-efficient MC-NOMA with imperfect channel state information. IEEE Trans. Commun. **65**(9), 3944–3961 (2017)
2. F. Zhou, N.C. Beaulieu, Z. Li, J. Si, P. Qi, Energy-efficient optimal power allocation for fading cognitive radio channels: ergodic capacity, outage capacity, and minimum-rate capacity. IEEE Trans. Wirel. Commun. **15**(4), 2741–2755 (2016)
3. D. Tse, P. Viswannath, *Fundamentals of Wireless Communication* (2005)
4. Z. Ding, Z. Yang, P. Fan, H.V. Poor, On the performance of non-orthogonal multiple access in 5G systems with randomly deployed users. IEEE Signal Process. Lett. **21**(12), 1501–1505 (2014)
5. Z. Ding, P. Fan, H.V. Poor, Impact of user pairing on 5G nonorthogonal multiple-access downlink transmissions. IEEE Trans. Veh. Technol. **65**(8), 6010–6023 (2016)
6. J. Men, J. Ge, Non-orthogonal multiple access for multiple-antenna relaying networks. IEEE Commun. Lett. **19**(10), 1686–1689 (2015)
7. Z. Yang, Z. Ding, Y. Wu, P. Fan, Novel relay selection strategies for cooperative NOMA. IEEE Trans. Veh. Technol. **66**(11), 10114–10123 (2017). https://doi.org/10.1109/TVT.2017.2752264

8. P. Xu, Z. Yang, Z. Ding, Z. Zhang, Optimal relay selection schemes for cooperative NOMA. IEEE Trans. Veh. Technol. **6**, 16 (2018)
9. Z. Ding, H. Dai, H. Vincent, Relay selection for cooperative NOMA. IEEE Wirel. Commun. Lett. **5**(4), 416–419 (2016)
10. J. Li, Y. Zhao, Radio environment map-based cognitive doppler spread compensation algorithms for high-speed rail broadband mobile communications. EURASIP J. Wirel. Commun. Netw. **263**, 2012 (2012)
11. S.L. Talbot, B. Farhang-Boroujeny, Time-varying carrier offsets in mobile OFDM. IEEE Trans. Commun. **57**(9), 2790–2798 (2009)
12. Z. Zhu, Z. Chu, Z. Wang, L. Lee, Outage constrained robust beamforming for secure broadcasting systems with energy harvesting. IEEE Trans. Wirel. Commun. **15**(11), 7610–7620 (2016)
13. P. Grover, A. Sahai, Shannon meets tesla: Wireless information and power transfer, in *IEEE International Symposium on Information Theory* (2010)
14. I. Krikidis, S. Timotheou, S. Nikolaou, G. Zheng, D.W.K. Ng, R. Schober, Simultaneous wireless information and power transfer in modern communication systems. IEEE Commun. Mag. **52**(11), 104–110 (2014)
15. R. Zhang, C.K. Ho, MIMO broadcasting for simultaneous wireless information and power transfer. IEEE Trans. Wirel. Commun. **12**(5), 1989–2001 (2013)
16. F. Zhou, Z. Chu, H. Sun, R.Q. Huang, L. Hanzo, Artificial noise aided secure cognitive beamforming for cooperative miso-noma using swipt. IEEE J. Sel. Areas Commun. **36**(4), 918–931 (2018)
17. J. Xu, L. Liu, R. Zhang, Multiuser MISO beamforming for simultaneous wireless information and power transfer. IEEE Trans. Signal Process. **62**(18), 4798–4810 (2014)
18. Y. Liu, Z. Ding, M. Elkashlan, H.V. Poor, Cooperative non-orthogonal multiple access with simultaneous wireless information and power transfer. IEEE J. Sel. Areas Commun. **34**(4), 938–953 (2016)
19. Y. Xu, C. Shen, Z. Ding, X. Sun, S. Yan, G. Zhu, Z. Zhong, Joint beamforming and power-splitting control in downlink cooperative SWIPT NOMA systems. IEEE Trans. Signal Process. **65**(18), 4874–4886 (2017)
20. Y. Yuan, P. Xu, Z. Yang, Z. Ding, Q. Chen, Joint robust beamforming and power-splitting ratio design in SWIPT-based cooperative NOMA systems with CSI uncertainty. IEEE Trans. Veh. Technol. **68**(3), 2386–2400 (2019)
21. F. Zhou, Z. Li, J. Cheng, Q. Li, J. Si, Robust AN-aided beamforming and power splitting design for secure MISO cognitive radio with SWIPT. IEEE Trans. Wirel. Commun. **16**(4), 2450–2464 (2017)
22. H. Wang, X. Xia, Enhancing wireless secrecy via cooperation: signal design and optimization. IEEE Commun. Mag. **53**(12), 47–53 (2015)
23. Y. Ju, H. Wang, T. Zheng, Q. Yin, Secure transmissions in millimeter wave systems. IEEE Trans. Commun. **65**(5), 2114–2127 (2017)
24. M. Moradikia, H. Bastami, A. Kuhestani, H. Behroozi, L. Hanzo, Cooperative secure transmission relying on the optimal power allocation in the presence of untrusted relays, a passive eavesdropper and hardware impairments. IEEE Access **7**, 116942–116964 (2019)
25. C. Wang, H.W. Ming, X. Xia, Hybrid opportunistic relaying and jamming with power allocation for secure cooperative networks. IEEE Trans. Wirel. Commun. **14**(2), 589–605 (2015)
26. Y. Liu, H. Chen, L. Wang, Physical layer security for next generation wireless networks: theories, technologies, and challenges. IEEE Commun. Surv. Tutor. **19**(1), 347–376 (2017)
27. F. Zhou, Z. Chu, Y. Wu, N.Al-Dhahir, P. Xiao, Enhancing PHY security of MISO NOMA SWIPT systems with a practical non-linear EH model, in *2018 IEEE International Conference on Communications Workshops (ICC Workshops)*, pp. 1–6 (IEEE, 2018)
28. D. Chen, Y. Cheng, W. Yang, J. Hu, Y. Cai, Physical layer security in cognitive untrusted relay networks. IEEE Access **6**, 7055–7065 (2018)
29. M.T. Mamaghani, Y. Hong, On the performance of low-altitude UAV-enabled secure af relaying with cooperative jamming and SWIPT. IEEE Access **7**, 153060–153073 (2019)
30. Z. Hu, D. Xie, M. Jin, L. Zhou, J. Li, Relay cooperative beamforming algorithm based on probabilistic constraint in SWIPT secrecy networks. IEEE Access **8**, 173999–174008 (2020)
31. K. Cao, B. Wang, H. Ding, L. Lv, R. Dong, T. Cheng, F. Gong, Improving physical layer security of uplink noma via energy harvesting jammers. IEEE Trans. Inf. Forensics Secur. **16**, 786–799 (2021)
32. A. Hasan, J.G. Andrews, The guard zone in wireless ad hoc networks. IEEE Trans. Wirel. Commun. **6**(3), 897–906 (2007)
33. Y. Zhang, H. Wang, Q. Yang, Z. Ding, Secrecy sum rate maximization in non-orthogonal multiple access. IEEE Commun. Lett. **20**(5), 930–933 (2016)
34. Q. Shi, C. Peng, W. Xu, M. Hong, Y. Cai, Energy efficiency optimization for MISO SWIPT systems with zero-forcing beamforming. IEEE Trans. Signal Process. **64**(4), 842–854 (2016)
35. Z. Ding, I. Krikidis, B. Sharif, H.V. Poor, Wireless information and power transfer in cooperative networks with spatially random relays. IEEE Trans. Wirel. Commun. **13**(8), 4440–4453 (2014)
36. Z. Chu, Z. Zhu, M. Johnston, S.Y. LeGoff, Simultaneous wireless information power transfer for MISO secrecy channel. IEEE Trans. Veh. Technol. **65**(9), 6913–6925 (2016)
37. S. Boyd, L. Vandenberghe, *Convex Optimization* (2004)
38. Z. Luo, W. Ma, M. So, Y. Ye, S. Zhang, Semidefinite relaxation of quadratic optimization problems. IEEE Signal Process. Mag. **27**(3), 20–34 (2010)

Publisher's Note